

Nussbaum Gain-Based Cone Angle Constrained Fault-Tolerant Attitude Control with Time-Varying Inertia

Srianish Vutukuri* Radhakant Padhi*

* Department of Aerospace Engineering, Indian Institute of Science, Bangalore, India (e-mail: padhi@iisc.ac.in)

Abstract: This paper proposes a robust adaptive attitude control law for handling a class of actuator faults in the presence of various challenges, such as time-varying inertia, attitude constraints, and input saturation. The proposed approach uses cone angles to represent orientation errors, which are constrained within a performance function to ensure desired transient and steady-state behaviour during reference tracking. Input saturation is approximated using a smooth hyperbolic tangent function. The Nussbaum gain technique is used to handle the unknown control coefficients, which guarantees uniformly ultimately bounded stability in the presence of uncertainties and disturbances. The paper also proposes a norm-based disturbance approximation to estimate the total uncertainty during the Lyapunov analysis. Numerical simulations demonstrate the effectiveness of the proposed control law.

Copyright © 2023 The Authors. This is an open access article under the CC BY-NC-ND license (<https://creativecommons.org/licenses/by-nc-nd/4.0/>)

Keywords: Robust adaptive control, Fault-tolerant control, Constrained control, Time-varying inertia, Barrier Lyapunov function.

1. INTRODUCTION

Attitude control of rigid bodies requires tracking a reference orientation while adhering to system constraints and ensuring safety. However, nonlinear dynamics, uncertainties, and disturbances make designing a control law challenging. In addition, the moment of inertia (MOI) matrix can vary significantly under actuator constraints. To overcome these challenges, stabilizing control laws were synthesized in the past (Zhang et al. (2021); Hou and Sun (2020)) using robust and adaptive control strategies. These approaches assume healthy actuator conditions, but irreversible actuator faults pose a safety hazard.

Recent Fault Tolerant Control (FTC) strategies (Gao et al. (2021b,a)) handle input saturation using Nussbaum gains and achieve desired transient and steady-state attitude tracking through a prescribed performance constraint (PPC) function. However, limited literature addresses redundancy in control actuation and complete actuator failures (Gao et al. (2021b); Hu et al. (2018)). Moreover, time-varying MOI presents a critical challenge in practice. The inertia matrix can change due to various factors such as payload mass variations and moving/deployable parts in the rigid body (Thakur et al. (2015)). There is a research gap in FTC that addresses these constraints while accommodating time-varying MOI.

In our recent work (Vutukuri et al. (2022)), physically meaningful cone angles were used to indicate orientation errors. This paper proposes an error transformation that imposes nonlinear constraints on quaternions while limiting the cone angles within a time-varying constraint. A smooth hyperbolic tangent function models the physical limitations of the actuators, and matrix operators handle time-varying MOI and associated uncertainty. The fea-

tures of the controller are 1.) The proposed controller minimizes total control effort and strictly meets time-varying attitude constraints, despite time-varying MOI, parameter variation, exogenous disturbances, a class of actuator faults, and input saturation. 2.) Closed-loop stability of all signals is guaranteed, and tracking errors remain uniformly ultimately bounded (UUB). 3.) The norm-based disturbance approximation reduces computational demand, and knowledge of uncertainty bounds is not required.

This paper uses $\mathbf{0}_q := [0; 0; 0; 1]^T$ to indicate the zero quaternion. $\|\bullet\|$ refers to a euclidean/induced second norm of a vector/matrix, and $\mathbf{I} \in \mathbb{R}^{3 \times 3}$ indicates the identity matrix. For a vector $\mathbf{x} = [x_1; x_2; x_3]^T \in \mathbb{R}^{3 \times 1}$, \mathbf{x}^\times denotes a skew-symmetric matrix given by

$$\mathbf{x}^\times = \begin{bmatrix} 0 & -x_3 & x_2 \\ x_3 & 0 & -x_1 \\ -x_2 & x_1 & 0 \end{bmatrix}$$

2. PROBLEM FORMULATION

2.1 Attitude Error Kinematics and Dynamics

Fig. (1a) shows the orientation of a rigid body frame, $\mathcal{B} = \{\hat{b}_1, \hat{b}_2, \hat{b}_3\}$, in an inertial frame, $\mathcal{I} = \{\hat{i}_1, \hat{i}_2, \hat{i}_3\}$. \mathcal{B} is placed at the center of mass, B , of the rigid body, and its orientation is represented by a unit quaternion $\mathbf{q} = [q_v^T; q_4]^T$ with vector and scalar parts $\mathbf{q}_v = [q_1; q_2; q_3]^T$ and q_4 , respectively. The angular velocity of \mathcal{B} with respect to \mathcal{I} , expressed in \mathcal{B} , is $\boldsymbol{\omega}$. A desired reference frame, $\mathcal{B}_r = \{\hat{b}_{1r}, \hat{b}_{2r}, \hat{b}_{3r}\}$, is placed at B , and its orientation with respect to \mathcal{I} is represented by the unit quaternion $\mathbf{q}_r = [q_{vr}^T; q_{4r}]^T$ with vector and scalar parts $\mathbf{q}_{vr} =$

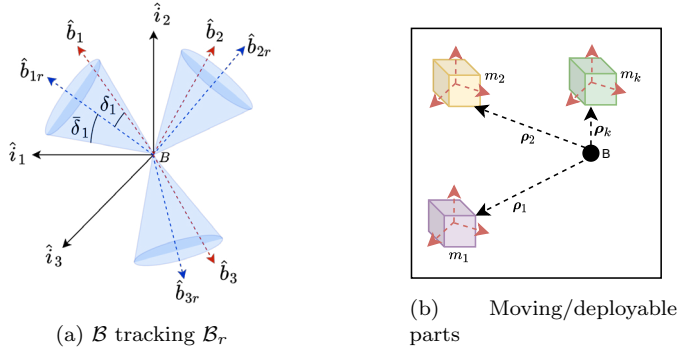


Figure 1. Reference frames and changing MOI.

$[q_{1r}; q_{2r}; q_{3r}]^T$ and q_{4r} , respectively. The angular velocity of \mathcal{B}_r with respect to \mathcal{I} , expressed in \mathcal{B}_r , is ω_r . The error quaternion, $\mathbf{q}_e = [q_{ve}^T; q_{4e}]^T$, is used to determine the relative orientation of \mathcal{B} with respect to \mathcal{B}_r as

$$\mathbf{q}_{ve} = -q_4 \mathbf{q}_{vr} + q_{4r} \mathbf{q}_v + \mathbf{q}_v \times \mathbf{q}_{vr}, \quad q_{4e} = q_4 q_{4r} + \mathbf{q}_v^T \mathbf{q}_{vr}$$

The angular velocity of \mathcal{B} relative to \mathcal{B}_r , expressed in \mathcal{B} , is $\omega_e = [\omega_{1e} \ \omega_{2e} \ \omega_{3e}]^T$ and obtained as $\omega_e = \omega - C_{\mathcal{B}_r}^{\mathcal{B}} \omega_r$. Here $C_{\mathcal{B}_r}^{\mathcal{B}}$ indicates the direction cosine matrix (DCM) that relates \mathcal{B}_r to \mathcal{B} and computed using, \mathbf{q}_e , as

$$C_{\mathcal{B}_r}^{\mathcal{B}} = (q_{4e}^2 - \mathbf{q}_{ve}^T \mathbf{q}_{ve}) \mathbf{I}_{3 \times 3} + 2 \mathbf{q}_{ve} \mathbf{q}_{ve}^T - 2 q_{4e} \mathbf{q}_{ve}^\times \quad (1)$$

The dynamics of \mathbf{q}_e and ω_e are obtained as

$$\dot{\mathbf{q}}_e = Q_e \omega_e, \quad \dot{\omega}_e = \dot{\omega} + \omega_e^\times C_{\mathcal{B}_r}^{\mathcal{B}} \omega_r - C_{\mathcal{B}_r}^{\mathcal{B}} \dot{\omega}_r \quad (2)$$

The matrix Q_e takes the form

$$Q_e = \frac{1}{2} \begin{bmatrix} q_{4e} \mathbf{I} + \mathbf{q}_{ve}^\times \\ -\mathbf{q}_{ve}^T \end{bmatrix}$$

Assumption 1. The states \mathbf{q} and ω are available. The desired angular velocity and its derivative are bounded quantities, i.e., $\|\omega_r\| < \bar{\omega}_r$ and $\|\dot{\omega}_r\| < \bar{\dot{\omega}}_r$ for all $t \geq 0$.

The dynamics associated with ω is

$$J \dot{\omega} = -\dot{J} \omega - \omega^\times J \omega + D(E \text{Sat}(\tau) + \tau_f) + \tau_e \quad (3)$$

$\text{Sat}(\tau) = [\text{sat}(\tau_1) \ \cdots \ \text{sat}(\tau_n)]^T \in \mathbb{R}^{n \times 1}$ is the control torque subjected to saturation constraints, where $\tau = [\tau_1; \cdots; \tau_n]^T \in \mathbb{R}^{n \times 1}$ is the commanded torque generated by $n > 3$ actuators. τ_f denotes a bounded faulty torque arising due to unexpected deviations of the actuators, and τ_e is an external disturbance torque acting on the rigid body. $D \in \mathbb{R}^{3 \times n}$ indicates the actuator distribution matrix, and $E = \text{diag}\{e_1 \ \cdots \ e_n\} \in \mathbb{R}^{n \times n}$ represents the control effectiveness matrix that denotes the health status of the actuators, where $0 \leq e_i \leq 1, \forall i = 1, \cdots, n$. The case $e_i = 1$ and $\tau_{if} = 0$ indicates that the i^{th} actuator is healthy, otherwise it is faulty. $J \in \mathbb{R}^{3 \times 3}$ indicates the MOI of the rigid body.

Assumption 2. Gao et al. (2021b); Shao et al. (2018): Actuators are mounted along \mathcal{B} such that $\text{rank}(D) = 3$ and for the entire duration $\text{rank}(DE) = 3$. The implication is that the number of completely failed actuators is never more than $n - 3$. When more than $n - 3$ actuators completely fail, $\text{rank}(E) < 3$, and $\text{rank}(DE) < 3$, causing under-actuation and making it challenging to track a reference attitude.

2.2 Modeling Parametric Uncertainties

Actuator misalignment introduces uncertainties in D as $D = D_n + \tilde{D}_n$, where D_n and \tilde{D}_n are the nominal and perturbed values of the distribution matrix, respectively. The rigid body may also have moving/deployable parts resulting in a time-dependent variation of J , explained in Thakur et al. (2015) as

$$J(t) = (J_n + \tilde{J}_n) + (J_{nm} + \tilde{J}_{nm}) \Psi(t) \quad (4)$$

here the constants $J_n, \tilde{J}_n \in \mathbb{R}^{3 \times 3}$ indicate a nominal and uncertain portion of the inertia matrix, respectively. The constant terms $J_{nm}, \tilde{J}_{nm} \in \mathbb{R}^{3 \times k}$ represent a nominal and uncertain mass matrix. The term $\Psi(t) \in \mathbb{R}^{k \times 3}$ is a well characterized time-dependent matrix. The number of moving parts is indicated by k .

Remark 1. Thakur et al. (2015): It is assumed that the position of center of mass, B , is unaffected by the moving parts. MOI modeling in Eq. (4) must ensure $J(t)$ remains symmetric and positive definite for all $t \geq 0$. To guarantee a physically possible distribution of mass, $J(t)$ must satisfy

$$\bar{J}_1 + \bar{J}_2 \geq \bar{J}_3, \quad \bar{J}_2 + \bar{J}_3 \geq \bar{J}_1, \quad \bar{J}_3 + \bar{J}_1 \geq \bar{J}_2 \quad \forall t \geq 0 \quad (5)$$

$\bar{J}_1, \bar{J}_2, \bar{J}_3$ indicate principal MOI. Terms in Eq. (4) are

$$\Psi(t) = \begin{bmatrix} \rho_1^T(t) \rho_1(t) \mathbf{I} - \rho_1(t) \rho_1^T(t) \\ \vdots \\ \rho_k^T(t) \rho_k(t) \mathbf{I} - \rho_k(t) \rho_k^T(t) \end{bmatrix} \quad (6)$$

$$(J_{nm} + \tilde{J}_{nm}) = [(m_{1n} + \tilde{m}_{1n}) \mathbf{I} \ \cdots \ (m_{kn} + \tilde{m}_{kn}) \mathbf{I}] \quad (7)$$

For all $i = 1, \cdots, k$ the moving part i has a nominal mass m_{in} , an associated uncertain component \tilde{m}_{in} that is located at a bounded position $\rho_i(t)$ relative to B .

2.3 Modeling Input Saturation

The input saturation function in Eq. (3) represents

$$\text{sat}(\tau_i) = \begin{cases} \bar{\tau}_i, & \text{if } \tau_i \geq \bar{\tau}_i \\ \tau_i, & \text{if } |\tau_i| < \bar{\tau}_i, \forall i = 1, \cdots, n \\ -\bar{\tau}_i, & \text{if } \tau_i \leq -\bar{\tau}_i \end{cases} \quad (8)$$

here, $\bar{\tau}_i$ denotes the maximum output torque provided by the i^{th} actuator. The saturation function is approximated using a smooth, tan-hyperbolic function as

$$\text{sat}(\tau_i) = \underbrace{\bar{\tau}_i \tanh\left(\frac{\tau_i}{\bar{\tau}_i}\right)}_{s_i(\tau_i)} + \tau_{is}$$

here, τ_{is} is the error resulting from tan-hyperbolic approximation and is bounded by $|\tau_{is}| \leq \bar{\tau}_i (1 - \tanh(1))$. Further, applying the mean-value theorem to $s_i(\tau_i)$

$$s_i(\tau_i) = s_i(0) + \left. \frac{\partial s_i}{\partial \tau_i} \right|_{\tau_i=\tau_i^*} (\tau_i - 0) \quad (9)$$

here τ_i^* lies between 0 and τ_i . By defining $s_i^* := \left. \frac{\partial s_i}{\partial \tau_i} \right|_{\tau_i=\tau_i^*}$,

Eq. (9) reduces to $\text{sat}(\tau_i) = s_i^* \tau_i + \tau_{is}$. Due to the nature of tan hyperbolic function, the term $s_i^* > 0$. Following similar saturation approximation along all the channels results in the following vector form

$$\text{Sat}(\tau) = S \tau + \tau_s \quad (10)$$

The unknown matrix $S = \text{diag}\{s_1^* \cdots s_n^*\} \in \mathbb{R}^{n \times n}$ is positive definite and the disturbance vector due to saturation approximation is indicated by $\tau_s = [\tau_{1s} \cdots \tau_{ns}]^T \in \mathbb{R}^{n \times 1}$. Substituting Eq. (10) into Eq. (3) results in

$$J\dot{\omega} = -\dot{J}\omega - \omega^\times J\omega + D_n U\tau + \tau_d$$

Note that $U = ES = \text{diag}\{u_1, \dots, u_n\} \in \mathbb{R}^{n \times n}$ is an unknown, *diagonal positive definite* matrix. A combined lumped disturbance term arising due to variation in distribution matrix, saturation approximation, actuator faults and external disturbances is indicated by

$$\tau_d := D_n(E\tau_s + \tau_f) + \tilde{D}_n(E \text{Sat}(\tau) + \tau_f) + \tau_e \quad (11)$$

Assumption 3. The terms, τ_s , τ_f , τ_e in Eq. (11) are unknown but bounded quantities. The saturation function in Eq. (8), the nominal distribution matrix, D_n , and its variation, \tilde{D}_n , are bounded quantities. This leads to the lumped disturbance term to be bounded as $0 < \|\tau_d\| < \bar{\tau}_d$.

2.4 General Time-varying Attitude Constraints

A set of angles, δ_i , $\forall i = 1, 2, 3$, that correspond to the angles between \hat{b}_i and \hat{b}_{ir} axes are subject to time-varying constraints as $\delta_i(t) < \bar{\delta}_i(t)$, $\forall i = 1, 2, 3$. The DCM in Eq. (1) allows the constraints to be transformed into

$$\begin{aligned} e_1 &:= q_{2e}^2 + q_{3e}^2 < \bar{e}_1, \quad e_2 := q_{1e}^2 + q_{3e}^2 < \bar{e}_2 \\ e_3 &:= q_{1e}^2 + q_{2e}^2 < \bar{e}_3 \end{aligned} \quad (12)$$

here $\bar{e}_i = (1 - \cos(\bar{\delta}_i))/2$, $\forall i = 1, 2, 3$. The set of \mathbf{q}_e that satisfy the constraints in Eq. (12) form an inclusion type set $\mathcal{U}_q := \{\mathbf{q}_e | e_i < \bar{e}_i \forall i = 1, 2, 3\}$.

Remark 2. When \mathcal{B} is perfectly aligned with \mathcal{B}_r , the cone angles $\delta_i = 0$, $\forall i = 1, 2, 3$, the quaternion $\mathbf{q}_e = \mathbf{0}_q$ and $\omega_e = \mathbf{0}_{3 \times 1}$. From Eq. (12), this results in $e_i = 0$, $\forall i = 1, 2, 3$. As \mathbf{q}_e and $-\mathbf{q}_e$ represent the same orientation, without loss of generality, the initial value of the scalar component is considered to be positive, i.e., $q_{4e}(0) > 0$. Tracking \mathcal{B}_r via the shortest path warrants $q_{4e}(t) > 0$ for all $t > 0$. Using Eq. (12), the constraint set \mathcal{U}_q in which \mathbf{q}_e evolves that ensures $q_{4e}(t) > 0$, must satisfy

$$\sum_{i=1}^3 q_{ie}^2 = 1 - q_{4e}^2 < \frac{\bar{e}_1 + \bar{e}_2 + \bar{e}_3}{2} < 1, \quad \forall t \geq 0 \quad (13)$$

Simplifying the right-hand side of Eq. (13) results in the requirement of inequality $\sum_{i=1}^3 \cos(\bar{\delta}_i(t)) > -1$.

2.5 Control Objective

To design a robust adaptive control law to achieve the following objectives despite actuator faults, time-varying MOI, orientation and input constraints, uncertain parameters and external disturbances. i) The rigid body must track the desired attitude, i.e., $\mathbf{q}_e \rightarrow \mathbf{0}_q$ and $\omega_e \rightarrow \mathbf{0}_{3 \times 1}$ while staying within the set \mathcal{U}_q . ii) All the closed-loop signals remain bounded.

3. PRELIMINARIES

Lemma 1. Tee et al. (2011) For a positive constant $k_z \in \mathbb{R}^+$, the following inequality $\log\left(\frac{k_z}{k_z - z}\right) \leq \frac{z}{k_z - z}$ holds for any $z \in [0, k_z)$.

Lemma 2. Tee et al. (2011) For a matrix $M \in \mathbb{R}^{n \times n}$, vector $\mathbf{x} \in \mathbb{R}^{n \times 1}$, $\|\mathbf{x}\|_i$ representing the i^{th} norm, the following inequalities hold $\|\mathbf{x}\|_\infty \leq \|\mathbf{x}\|_2 \leq \|\mathbf{x}\|_1$, $\lambda_{\min}(M)\mathbf{x}^T \mathbf{x} \leq \mathbf{x}^T M \mathbf{x} \leq \lambda_{\max}(M)\mathbf{x}^T \mathbf{x}$, $\|M\mathbf{x}\|_2 \leq \|M\|_2 \|\mathbf{x}\|_2 \leq \|M\|_F \|\mathbf{x}\|_2$. Here $\lambda_{\min}(\bullet)$ and $\lambda_{\max}(\bullet)$ denote the minimum and maximum eigenvalues of the matrix and $\|\bullet\|_F$ denotes the Frobenius norm of the matrix. Consider two vectors $\mathbf{x}, \mathbf{y} \in \mathbb{R}^{n \times 1}$. The inequality $(\mathbf{x} - \mathbf{y})^T (\mathbf{x} - \mathbf{y}) \geq 0$ leads to $\mathbf{x}^T \mathbf{y} \leq \frac{\mathbf{x}^T \mathbf{x}}{2} + \frac{\mathbf{y}^T \mathbf{y}}{2}$.

Lemma 3. For a vector $\mathbf{x} = [x_1 \ x_2 \ x_3]^T \in \mathbb{R}^{3 \times 1}$ and \tilde{J}_n representing the symmetric uncertain portion of MOI in Eq. (4), there exists a linear operator $\mathcal{L}_1\{\bullet\} : \mathbb{R}^{3 \times 1} \rightarrow \mathbb{R}^{3 \times 6}$ such that $\tilde{J}_n \mathbf{x} = \mathcal{L}_1\{\mathbf{x}\} \boldsymbol{\theta}_1$ with

$$\mathcal{L}_1\{\mathbf{x}\} := \begin{bmatrix} x_1 & x_2 & x_3 & 0 & 0 & 0 \\ 0 & x_1 & 0 & x_2 & x_3 & 0 \\ 0 & 0 & x_1 & 0 & x_2 & x_3 \end{bmatrix}_{3 \times 6} \quad (14)$$

$$\boldsymbol{\theta} = [\tilde{J}_{n11} \ \tilde{J}_{n12} \ \tilde{J}_{n13} \ \tilde{J}_{n22} \ \tilde{J}_{n23} \ \tilde{J}_{n33}]^T \quad (15)$$

here $\tilde{J}_{n_{ij}}$ indicates the element in row i and column j of \tilde{J}_n . For a vector $\mathbf{x} = [x_1 \ \cdots \ x_{3k}]^T \in \mathbb{R}^{3k \times 1}$ and the uncertain mass matrix $\tilde{J}_{nm} = [\tilde{m}_{1n} \mathbf{I} \ \cdots \ \tilde{m}_{kn} \mathbf{I}] \in \mathbb{R}^{3 \times 3k}$ in Eq. (7), there exists a linear operator $\mathcal{L}_2\{\bullet\} : \mathbb{R}^{3k \times 1} \rightarrow \mathbb{R}^{3 \times k}$ such that $\tilde{J}_{nm} \mathbf{x} = \mathcal{L}_2\{\mathbf{x}\} \boldsymbol{\theta}_2$ with

$$\mathcal{L}_2\{\mathbf{x}\} := \begin{bmatrix} x_1 & x_4 & & x_{3k-2} \\ x_2 & x_5 & \cdots & x_{3k-1} \\ x_3 & x_6 & & x_{3k} \end{bmatrix}_{3 \times k} \quad \boldsymbol{\theta}_2 = [\tilde{m}_{1n} \ \cdots \ \tilde{m}_{kn}]^T \quad (16)$$

Lemma 4. Tee et al. (2011) For a $\delta > 0$ and $x \in \mathbb{R}$, the result $0 \leq |x| - x \tanh(x/\delta) \leq \alpha\delta$, $\alpha = 0.2785$ holds.

3.1 Nussbaum-type Function

A continuous function $N(\bullet)$ is called a Nussbaum-type function if it satisfies the following properties

$$\lim_{l \rightarrow +\infty} \sup \frac{1}{l} \int_0^l N(\chi) d\chi = +\infty, \quad \lim_{l \rightarrow +\infty} \inf \frac{1}{l} \int_0^l N(\chi) d\chi = -\infty$$

In this paper, with multiple inputs and outputs, the Nussbaum-type function inspired from Gao et al. (2021b,a) is selected as

$$N(\chi) = e^{\frac{\chi^2}{2}} (\chi^2 + 2) \sin(\chi) + 1 \quad (17)$$

Lemma 5. Gao et al. (2021b,a) Let $V(\bullet)$ and $\chi_i(\bullet)$ be smooth functions defined on $[0 \ t_f)$ with $V(t) \geq 0$, $\chi_i(0) = 0 \ \forall i = 1, \dots, n$. If $N_i(\bullet)$ is a Nussbaum-type function in Eq. (17) with the following inequality satisfied

$$V(t) \leq c_0 + e^{-c_1 t} \sum_{i=1}^n \int_0^t (-u_i(\nu) N_i(\chi_i(\nu)) + 1) \dot{\chi}_i(\nu) e^{c_1 \nu} d\nu$$

here $c_1 > 0$, $u_i(t)$ is a time-varying parameter that belongs to the unknown set $I := [u_i^- \ u_i^+]$ with $0 \notin I$ and c_0 is a bounded constant. Then $V(t)$, $\chi_i(t)$ and $\sum_{i=1}^n \int_0^t u_i(\nu) N_i(\chi_i(\nu)) \dot{\chi}_i(\nu) d\nu$ are bounded on $[0 \ t_f)$.

3.2 Barrier Lyapunov Function

Four output errors are chosen as e_1, e_2, e_3 in Eq. (12) and $e_4 = q_{4e} - 1$. The Lyapunov function is designed as

$$V_q = \frac{k_q}{2} \left(\sum_{i=1}^3 \log\left(\frac{\bar{e}_i}{\bar{e}_i - e_i}\right) + e_4^2 \right) \quad (18)$$

here $k_q > 0$ and $\log(\bullet)$ denotes the natural logarithm. The outputs $e_i, \forall i = 1, 2, 3$ that require strict enforcement of constraints are incorporated using BLFs. The Lyapunov function defined in Eq. (18) is smooth, non-negative and strictly convex within the set \mathcal{U}_q and admits a unique global minimum at $\mathbf{q}_e = \mathbf{0}_q \in \mathcal{U}_q$.

4. CONTROLLER SYNTHESIS - BACKSTEPPING

Step 1: A steady state tracking error for \mathbf{q}_e is defined as $\mathbf{z}_q = \mathbf{q}_e - \mathbf{0}_q$. An angular velocity tracking error, \mathbf{z}_ω , is defined as the difference between $\boldsymbol{\omega}_e$ and a stabilizing control, $\boldsymbol{\xi}$, as $\mathbf{z}_\omega = [z_{1\omega} \ z_{2\omega} \ z_{3\omega}]^T = \boldsymbol{\omega}_e - \boldsymbol{\xi}$. The term, $\boldsymbol{\xi} \in \mathbb{R}^{3 \times 1}$, is designed as

$$\boldsymbol{\xi} = \left(-\tilde{k}_q - \bar{k}_q(t) \right) [q_{1e}/q_{4e} \ q_{2e}/q_{4e} \ q_{3e}/q_{4e}]^T \quad (19)$$

here the constant $\tilde{k}_q > 0$ and the time-varying constant $\bar{k}_q(t) > 0$ is designed later. Using \mathbf{z}_q and \mathbf{z}_ω , derivative of V_q in Eq. (18) is

$$\dot{V}_q = -\frac{\tilde{k}_q k_q}{2} \left(\sum_{i=1}^3 \frac{e_i}{\bar{e}_i - e_i} \right) - \frac{k_q \tilde{k}_q e_4^2 (1 + q_{4e})}{2q_{4e}} \dots + \mathbf{z}_\omega^T \underbrace{Q_e^T K_q \mathbf{z}_q}_{\mathbf{v}_{k_1}} + v_s \quad (20)$$

the scalar term v_s is denoted by

$$v_s = \frac{-k_q \tilde{k}_q e_4^2 (1 + q_{4e})}{2q_{4e}} - \frac{k_q}{2} \sum_{i=1}^3 \left(\tilde{k}_q + \frac{\dot{\bar{e}}_i}{\bar{e}_i} \right) \left(\frac{e_i}{\bar{e}_i - e_i} \right) \quad (21)$$

the matrix K_q is *diagonal* and *positive definite* in \mathcal{U}_q with $K_q(1, 1) = \frac{k_q}{\bar{e}_3 - e_3} + \frac{k_q}{\bar{e}_2 - e_2}$, $K_q(2, 2) = \frac{k_q}{\bar{e}_1 - e_1} + \frac{k_q}{\bar{e}_3 - e_3}$, $K_q(3, 3) = \frac{k_q}{\bar{e}_1 - e_1} + \frac{k_q}{\bar{e}_2 - e_2}$, $K_q(4, 4) = k_q$.

Remark 3. To ensure the validity of Eq. (19), the condition $q_{4e} \neq 0$ must be valid $\forall t \geq 0$. Hence a mild restriction is placed on the initial condition such that $q_{4e}(t_0) \neq 0$, and the subsequent adaptive control law must ensure $q_{4e} \neq 0 \ \forall t > 0$. This is feasible when the quaternion error always lies within the feasible set, \mathcal{U}_q , in which from Remark (2), $q_{4e} > 0$ is guaranteed.

Step 2: Choosing an augmented Lyapunov function, V_T

$$V_T = V_q + V_\omega + V_b, \quad V_\omega = \frac{\mathbf{z}_\omega^T J \mathbf{z}_\omega}{2}, \quad V_b = \frac{\tilde{\mathbf{b}}^T \tilde{\mathbf{b}}}{2\eta} \quad (22)$$

The term J indicates MOI matrix, $\tilde{\mathbf{b}}$ and $\eta > 0$ indicate the error in approximating the ideal weights and learning rate. The derivative \dot{V}_ω invoking Lemma (3) is

$$\dot{V}_\omega = \mathbf{z}_\omega^T (\mathbf{v}_{k_2} + D_n U \boldsymbol{\tau} + \boldsymbol{\tau}_d + V_1 \boldsymbol{\theta}_1 + V_2 \boldsymbol{\theta}_2) \quad (23)$$

here, the vector \mathbf{v}_{k_2} represents

$$\mathbf{v}_{k_2} = -\boldsymbol{\omega}^\times J_{nt} \boldsymbol{\omega} + J_{nt} \left(\boldsymbol{\omega}_e^\times C_{B_r}^B \boldsymbol{\omega}_r - C_{B_r}^B \dot{\boldsymbol{\omega}}_r - \dot{\boldsymbol{\xi}} \right) \dots + \dot{J}_{nt} \left(\frac{\mathbf{z}_\omega}{2} - \boldsymbol{\omega} \right) \quad (24)$$

The term $J_{nt} = J_n + J_{nm} \Psi(t)$ indicates the total nominal part of MOI and $\dot{J}_{nt} = J_{nm} \dot{\Psi}(t)$. The matrices V_1, V_2 and vectors $\boldsymbol{\theta}_1, \boldsymbol{\theta}_2$ represent

$$V_1 = -\boldsymbol{\omega}^\times \mathcal{L}_1 \{ \boldsymbol{\omega} \} + \mathcal{L}_1 \{ \boldsymbol{\omega}_e^\times C_{B_r}^B \boldsymbol{\omega}_r - C_{B_r}^B \dot{\boldsymbol{\omega}}_r - \dot{\boldsymbol{\xi}} \} \quad (25)$$

$$V_2 = -\boldsymbol{\omega}^\times \mathcal{L}_2 \{ \Psi(t) \boldsymbol{\omega} \} + \mathcal{L}_2 \left\{ \dot{\Psi}(t) \left(\frac{(\boldsymbol{\omega}_e - \boldsymbol{\xi})}{2} - \boldsymbol{\omega} \right) \right\} \dots + \mathcal{L}_2 \left\{ \Psi(t) \left(\boldsymbol{\omega}_e^\times C_{B_r}^B \boldsymbol{\omega}_r - C_{B_r}^B \dot{\boldsymbol{\omega}}_r - \dot{\boldsymbol{\xi}} \right) \right\} \quad (26)$$

$$\boldsymbol{\theta}_1 = [\tilde{J}_{n_{11}} \ \tilde{J}_{n_{12}} \ \tilde{J}_{n_{13}} \ \tilde{J}_{n_{22}} \ \tilde{J}_{n_{23}} \ \tilde{J}_{n_{33}}]^T \quad (27)$$

$$\boldsymbol{\theta}_2 = [\tilde{m}_{1n} \ \dots \ \tilde{m}_{kn}]^T \quad (28)$$

Assumption 4. The perturbation in MOI and mass of the moving/deployable parts are bounded quantities. Hence the following relation holds, $0 < \|\boldsymbol{\theta}_i\| < \bar{\theta}_i, \forall i = 1, 2$

Using Eq. (20) and Eq. (23) the derivative of the combined Lyapunov function, V_T , is

$$\dot{V}_T = -\frac{\tilde{k}_q k_q}{2} \left(\sum_{i=1}^3 \frac{e_i}{\bar{e}_i - e_i} \right) - \frac{k_q \tilde{k}_q e_4^2 (1 + q_{4e})}{2q_{4e}} + v_s \dots + \mathbf{z}_\omega^T \mathbf{v}_{k_1} + \mathbf{z}_\omega^T \mathbf{v}_{k_2} + \mathbf{z}_\omega^T D_n U \boldsymbol{\tau} \dots + \mathbf{z}_\omega^T V_1 \boldsymbol{\theta}_1 + \mathbf{z}_\omega^T V_2 \boldsymbol{\theta}_2 + \mathbf{z}_\omega^T \boldsymbol{\tau}_d - \frac{\tilde{\mathbf{b}}^T \dot{\tilde{\mathbf{b}}}}{\eta} \quad (29)$$

Using Assumption (4), Assumption (3) and Lemma (2), the following term is further expanded as

$$\mathbf{z}_\omega^T (V_1 \boldsymbol{\theta}_1 + V_2 \boldsymbol{\theta}_2 + \boldsymbol{\tau}_d) \leq \|\mathbf{z}_\omega\|_1 \left(\sum_{i=1}^2 \|V_i\|_F \bar{\theta}_i + \bar{\tau}_d \right) \quad (30)$$

An ideal weight vector, \mathbf{b} , and a regression vector, Φ , are defined that exactly model the lumped uncertainties and disturbances in Eq. (30) as $\mathbf{b}^T \Phi$ where $\mathbf{b} = [\bar{\theta}_1 \ \bar{\theta}_2 \ \bar{\tau}_d]^T$, $\Phi = [\|V_1\|_F \ \|V_2\|_F \ 1]^T$. Further, as long as the error quaternion (\mathbf{q}_e) lies within the feasible set (\mathcal{U}_q), we have $q_{4e} > 0$. Consequently from Eq. (20) the following observations are deduced i.) $(1 + q_{4e})/q_{4e} > 2$ ii) The constant \tilde{k}_q in v_s is designed as a time-varying parameter such that $\tilde{k}_q + \dot{\bar{e}}_i/\bar{e}_i > 0, \forall i = 1, 2, 3$. One possibility that satisfies the criterion is

$$\tilde{k}_q = \sqrt{\frac{\dot{\bar{e}}_1^2}{\bar{e}_1^2} + \frac{\dot{\bar{e}}_2^2}{\bar{e}_2^2} + \frac{\dot{\bar{e}}_3^2}{\bar{e}_3^2}} + k_\delta, \quad k_\delta > 0 \quad (31)$$

here k_δ is a small positive value introduced to ensure the derivative of \tilde{k}_q in $\dot{\boldsymbol{\xi}}$ exists despite the derivative of all the output error constraints, $\bar{e}_i, \forall i = 1, 2, 3$, are zero. These observations lead to the scalar $v_s \leq 0$ within the feasible set \mathcal{U}_q . Further, applying Lemma (1), the Lyapunov derivative in Eq. (29) is simplified as

$$\dot{V}_T \leq -\tilde{k}_q V_q + \mathbf{z}_\omega^T (\mathbf{v}_{k_1} + \mathbf{v}_{k_2}) + \|\mathbf{z}_\omega\|_1 \mathbf{b}^T \Phi + \mathbf{z}_\omega^T D_n U \boldsymbol{\tau} - \frac{\tilde{\mathbf{b}}^T \dot{\tilde{\mathbf{b}}}}{\eta}$$

The control laws are designed as

$$\boldsymbol{\tau} = \bar{N}(\boldsymbol{\chi}) \left(D_n^T (D_n D_n^T)^{-1} \right) \boldsymbol{\psi} \quad (32)$$

$$\boldsymbol{\psi} = -\mathbf{v}_{k_1} - \mathbf{v}_{k_2} - \tilde{k}_\omega \mathbf{z}_\omega - \hat{\mathbf{b}}^T \Phi \text{Tanh} \left(\frac{\mathbf{z}_\omega}{\varphi} \right) \quad (33)$$

here $\hat{\mathbf{b}} = \mathbf{b} - \tilde{\mathbf{b}}$ indicates the approximated weight vector. The term $\text{Tanh}(\bullet) \in \mathcal{R}^{3 \times 1}$ represents element-by-element hyperbolic tangent function as

$$\text{Tanh} \left(\frac{\mathbf{z}_\omega}{\varphi} \right) = \left[\tanh \left(\frac{z_{1\omega}}{\varphi} \right) \ \tanh \left(\frac{z_{2\omega}}{\varphi} \right) \ \tanh \left(\frac{z_{3\omega}}{\varphi} \right) \right]^T \quad (34)$$

In Eq. (32), the term $\bar{N}(\boldsymbol{\chi}) := \text{diag}\{N(\chi_1) \ \dots \ N(\chi_n)\} \in \mathbb{R}^{n \times n}$ represents the diagonal Nussbaum gain matrix with each element representing the Nussbaum-type function defined in Eq. (17). The vector $\boldsymbol{\chi} = [\chi_1 \ \dots \ \chi_n]^T \in \mathbb{R}^{n \times 1}$

represents the arguments of the Nussbaum-type function. The pseudo-inverse part of Eq. (32) is denoted by $\bar{D}_n := D_n^T (D_n D_n^T)^{-1} \in \mathbb{R}^{n \times 3}$ and row vector $i, \forall i = 1, \dots, n$ of matrix \bar{D}_n is indicated by $\bar{d}_i \in \mathbb{R}^{3 \times 1}$. Similarly, the column vector $i, \forall i = 1, \dots, n$ of matrix D_n is indicated by $\mathbf{d}_i \in \mathbb{R}^{3 \times 1}$. From the identity $D_n \bar{D}_n = \mathbf{I}$, the equation $\sum_{i=1}^n \mathbf{d}_i \bar{d}_i^T = \mathbf{I}$ holds. Expanding the term $\|\mathbf{z}_\omega\|_1 = \sum_{i=1}^3 |z_{i\omega}|$, by adding and subtracting the terms $\tilde{k}_\omega \mathbf{z}_\omega^T \mathbf{z}_\omega, \mathbf{z}_\omega^T \hat{\mathbf{b}}^T \Phi \text{Tanh}\left(\frac{\mathbf{z}_\omega}{\varphi}\right)$ and substituting Eq. (32) and Eq. (33) into the total Lyapunov derivative results in

$$\dot{V}_T \leq -\tilde{k}_q V_q - \tilde{k}_\omega \mathbf{z}_\omega^T \mathbf{z}_\omega - \mathbf{z}_\omega^T \boldsymbol{\psi} + \left(\sum_{i=1}^3 |z_{i\omega}|\right) \mathbf{b}^T \Phi - \frac{\tilde{\mathbf{b}}^T \hat{\mathbf{b}}}{\eta} \dots - \hat{\mathbf{b}}^T \Phi \text{Tanh}\left(\frac{\mathbf{z}_\omega}{\varphi}\right) + \mathbf{z}_\omega^T \left(\sum_{i=1}^n u_i N(\chi_i) \mathbf{d}_i \bar{d}_i^T\right) \boldsymbol{\psi} \quad (35)$$

Further, manipulating the term $\mathbf{z}_\omega^T \boldsymbol{\psi} := \mathbf{z}_\omega^T \left(\sum_{i=1}^n \mathbf{d}_i \bar{d}_i^T\right) \boldsymbol{\psi}$ and designing the adaptive laws as

$$\dot{\chi}_i = -\gamma_i \mathbf{z}_\omega^T \mathbf{d}_i \bar{d}_i^T \boldsymbol{\psi} \quad \forall i = 1, \dots, n \text{ and } \chi_i(0) = 0 \quad (36)$$

$$\dot{\hat{\mathbf{b}}} = \eta \left(\Phi \mathbf{z}_\omega^T \text{Tanh}\left(\frac{\mathbf{z}_\omega}{\varphi}\right) - \sigma \hat{\mathbf{b}} \right), \varphi = \mu / (1 + \|\Phi\|_\infty) \quad (37)$$

here constant $\sigma > 0$ indicates a stabilizing term, $\mu > 0$ and $\gamma_i, \eta > 0$ represent learning rates. Substituting Eq. (36) and Eq. (37) into Eq. (35) and invoking Lemma (2)

$$\dot{V}_T \leq -\tilde{k}_q V_q - \tilde{k}_\omega \mathbf{z}_\omega^T \mathbf{z}_\omega - \sigma \frac{\tilde{\mathbf{b}}^T \hat{\mathbf{b}}}{2} + \sum_{i=1}^n \frac{1}{\gamma_i} (-u_i N(\chi_i) + 1) \dot{\chi}_i \dots + \sigma \frac{\mathbf{b}^T \hat{\mathbf{b}}}{2} + \mathbf{b}^T \Phi \sum_{i=1}^3 \left(|z_{i\omega}| - z_{i\omega} \tanh\left(\frac{z_{i\omega}}{\varphi}\right) \right) \quad (38)$$

Applying Lemma (4) and the inequality $\Phi_i / (1 + \|\Phi\|_\infty) \leq 1$, the final term in Eq. (38) is

$$\mathbf{b}^T \Phi \sum_{i=1}^3 \left(|z_{i\omega}| - z_{i\omega} \tanh\left(\frac{z_{i\omega}}{\varphi}\right) \right) \leq 3\alpha\mu \left(\sum_{i=1}^2 \bar{\theta}_i + \bar{\tau}_d \right) \quad (39)$$

Substituting Eq. (39) into Eq. (38) leads to

$$\dot{V}_T \leq -k_d V_T + k_c + \sum_{i=1}^n \frac{1}{\gamma_i} (-u_i N(\chi_i) + 1) \dot{\chi}_i \quad (40)$$

here, $k_d = \min\{\tilde{k}_q, 2k_\omega / \lambda_{\max}(J), \sigma\eta\} > 0$ and $k_c = \sigma \frac{\mathbf{b}^T \hat{\mathbf{b}}}{2} + 3\alpha\mu \left(\sum_{i=1}^2 \bar{\theta}_i + \bar{\tau}_d \right) > 0$.

Remark 4. Gao et al. (2021b) The individual Nussbaum gains $N(\chi)$ in Eq. (17) are designed such that when the argument $\chi(t_0) = 0, \dot{\chi}(t) = 0 \forall t$, the resulting Nussbaum gain matrix $N(\boldsymbol{\chi})$ in Eq. (32) simplifies to an identity matrix. Then the remaining term, $\left(D_n^T (D_n D_n^T)^{-1}\right) \boldsymbol{\psi}$, is a standard control-norm minimizing torque synthesized for an unsaturated actuator with no faults.

4.1 Stability Analysis of the Closed-loop System

Theorem 1. Under the Assumptions (1)-(3) together with the control and adaptive laws synthesized in Eqs. (32), (33), (36) and (37) the constrained reference attitude tracking is achieved with the following conclusions 1.) All variables of the closed-loop system are bounded. 2.) The cone-angles, $\delta_i(t) \forall i = 1, 2, 3$, evolve strictly within the predefined constraint set \mathcal{U}_q and hence the condition $q_{4e} > 0$ holds.

Proof 1. Multiplying both sides of Eq. (40) by $e^{k_d t}$ and integrating the resulting expression over $[0 t]$ results in

$$V_T(t) \leq V_T(0) e^{-k_d t} + \frac{k_c}{k_d} \dots \sum_{i=1}^n \frac{1}{\gamma_i} \int_0^t (-u_i(\nu) N_i(\chi_i(\nu)) + 1) \dot{\chi}_i(\nu) e^{k_d(\nu-t)} d\nu \quad (41)$$

In Eq. (41), as the term $V_T(0) e^{-k_d t} + k_c/k_d \leq V_T(0) + k_c/k_d$ and $0 < u_i < 1$, from Lemma (5), the Nussbaum argument, $\chi_i(t)$, the term $\sum_{i=1}^n \frac{1}{\gamma_i} \int_0^t u_i(\nu) N_i(\chi_i(\nu)) \dot{\chi}_i(\nu) d\nu$ and the Lyapunov function, $V_T(t)$, are bounded on $[0 t_f)$. From Eq. (22), the boundedness of V_T leads to the individual positive definite functions V_q, V_ω and V_b to be bounded. This implies, with the initial attitude inside \mathcal{U}_b , the errors satisfy $e_i(t) < \bar{e}_i(t) \forall i = 1, 2, 3$ and the variables e_4, \mathbf{z}_ω and $\hat{\mathbf{b}}$ are bounded on $[0 t_f)$. The definition of $e_i, \forall i = 1, 2, 3$ in Eq. (12) and the relation $q_{4e} = e_4 + 1$ implies q_e remains bounded. The stabilizing function $\boldsymbol{\xi}$ in Eq. (19), that is a function of q_e stays bounded. The angular velocity error $\boldsymbol{\omega}_e = \mathbf{z}_\omega + \boldsymbol{\xi}$ remains a bounded value. Further, using Eq. (2) and Eq. (3), the bounds on q_r and $\boldsymbol{\omega}_r$ from Assumption (1) leads to q and $\boldsymbol{\omega}$ to be bounded. Therefore all signals in the closed-loop system remain bounded. Further, in Eq. (41), within the interval $0 \leq \nu \leq t$, the term $e^{k_d(\nu-t)} \leq 1$ and the term $\int_0^t \dot{\chi}_i(\nu) d\nu$ remains bounded as χ_i is bounded. Therefore, the bound on $\sum_{i=1}^n \int_0^t \frac{1}{\gamma_i} (-u_i(\nu) N_i(\chi_i(\nu)) + 1) \dot{\chi}_i(\nu) e^{k_d(\nu-t)} d\nu$ is denoted by $k_e > 0$. Then Eq. (41) simplifies to $V_T(t) \leq V_T(0) e^{-k_d t} + k_e + \frac{k_c}{k_d}$. The combined Lyapunov function is upper bounded by $\bar{V}_T = V_T(0) + k_e + \frac{k_c}{k_d}$. In Eq. (22), the inequality $V_q \leq V_T \leq \bar{V}_T$ always holds. This leads to

$$e_i(t) \leq \bar{e}_i(t) \left(1 - e^{\left(\frac{-2\bar{V}_T}{k_q}\right)} \right) \quad \forall i = 1, 2, 3 \quad (42)$$

From Eq. (42) it is clear that the tracking errors satisfy $e_i < \bar{e}_i \forall i = 1, 2, 3$ thereby strictly remaining within the set \mathcal{U}_q in which from Remark (2), $q_{4e} > 0$ holds. This implies the cone angles evolve within their respective constraints, i.e., $\delta_i(t) < \bar{\delta}_i(t) \forall i = 1, 2, 3$. Further, notice, as $t \rightarrow \infty$, the combined Lyapunov function satisfies $V_T(t_\infty) \leq k_f := k_e + \frac{k_c}{k_d}$. This implies the tracking errors are uniformly ultimately bounded as

$$e_i(t_\infty) \leq \bar{e}_i(t_\infty) \left(1 - e^{\left(\frac{-2k_f}{k_q}\right)} \right), \quad i = 1, 2, 3 \quad (43)$$

5. NUMERICAL SIMULATION

A satellite is commanded to track a desired attitude with orientation constraints under actuator faults and saturation. While doing so, its antennas are simultaneously commanded to spread out to establish communication. The nominal and perturbed parameters in Eq. (4) are

$$J_n = \begin{bmatrix} 30 & 1 & 0.5 \\ 1 & 20 & 3 \\ 0.5 & 3 & 10 \end{bmatrix}, \tilde{J}_n = \begin{bmatrix} 3 & 0.1 & -0.05 \\ 0.1 & 2 & 0.3 \\ -0.05 & 0.3 & 1 \end{bmatrix}$$

$$m_{1n} = 5, \tilde{m}_{1n} = 0.5, m_{2n} = 5, \tilde{m}_{2n} = 0.5$$

$$\boldsymbol{\rho}_1(t) = 0.15 (0.3\kappa t + 0.1 \sin(t)) \begin{bmatrix} 0\hat{b}_1 & 1\hat{b}_2 & 0\hat{b}_3 \end{bmatrix}^T$$

$$\boldsymbol{\rho}_2(t) = 0.15 (0.3\kappa t + 0.1 \sin(t)) \begin{bmatrix} 0\hat{b}_1 & 0\hat{b}_2 & 1\hat{b}_3 \end{bmatrix}^T$$

Here $\kappa = 1$ if $t \leq 20$ sec else $\kappa = 20/t$ otherwise. All the parameters are in S.I units. The nominal and perturbed mass together with the position of antennas from COM are indicated by m_{in} , \tilde{m}_{in} and ρ_i , respectively. The desired attitude that needs to be tracked is

$$\mathbf{q}_r(t_0) = [0 \ 0 \ 0 \ 1]^T$$

$$\boldsymbol{\omega}_r(t) = 0.025 [\sin(0.1\pi t) \ \cos(0.1\pi t) \ \sin(0.1\pi t)]^T \text{ rad/s}$$

The satellite starts with the following initial condition

$$\mathbf{q}(t_0) = [0.3 \ -0.2 \ 0.2 \ 0.9110]^T, \boldsymbol{\omega}(t) = [0.1 \ -0.05 \ -0.05]^T \text{ rad/s}$$

While tracking \mathcal{B}_r the cone angles, $\delta_i, \forall i = 1, 2, 3$ are constrained to evolve within a predefined PPC as $\bar{\delta}_i(t) = \bar{\delta}_{is} + (\bar{\delta}_{i0} - \bar{\delta}_{is})e^{-\frac{t}{t_c}}$. The parameters are chosen as $\bar{\delta}_{i0} = 60^\circ$, $\bar{\delta}_{is} = 0.05^\circ$, $t_c = 3$ sec. A bounded external disturbance torque on the satellite in \mathcal{B} frame is

$$\boldsymbol{\tau}_e = 10^{-2} \times [5 \cos(0.5\pi t) \ -3 \sin(0.3\pi t) \ 4 \sin(0.4\pi t)]^T \text{ N-m}$$

The satellite is controlled using four actuators arranged in a pyramidal structure. Each actuator makes an angle $\theta_i = \theta_{in} + \tilde{\theta}_{in}$ with \hat{b}_3 axis and its projection on $\hat{b}_1 - \hat{b}_2$ plane makes an angle $\phi_i = \phi_{in} + \tilde{\phi}_{in}$ with \hat{b}_1 axis. The nominal and perturbed orientation values are $\theta_{in} = 45^\circ$, $\tilde{\theta}_{in} = (-1)^{i+1}5^\circ$, $\phi_{in} = (i-1) \times 90^\circ - 45^\circ$, $\tilde{\phi}_{in} = (-1)^{i+1}5^\circ$, $\forall i = 1, 2, 3, 4$. The i^{th} column, $\mathbf{d}_i \forall i = 1, 2, 3, 4$ of the nominal matrix, $\mathbf{D}_n \in \mathcal{R}^{3 \times 4}$, is

$$\mathbf{d}_i = [\sin(\theta_{in})\cos(\phi_{in}) \ \sin(\theta_{in})\sin(\phi_{in}) \ \cos(\theta_{in})]^T$$

The actuators are faulty that lead to the diagonal elements of the effectiveness matrix as $e_1 = 0.7 + 0.09 \sin(0.05t)$, $e_2 = 0.6 + 0.1 \cos(0.08t)$, $e_3 = 0.4 + 0.08 \cos(0.06t)$, $e_4 = 0.6 + 0.07 \cos(0.07t)$. After $t \geq 40$ sec, the third actuator fails completely, i.e., $e_3 = 0$. During the entire faulty duration the system remains fully actuated, i.e., Assumption (2) is verified to hold. The corresponding deviation torque in N-m is $\tau_{1f} = 0.01$, $\tau_{2f} = -0.03 + 0.03e^{-0.5t}$, $\tau_{3f} = -0.02 + 0.02e^{-t}$, $\tau_{4f} = 0.015$. The controller constants are selected as $k_q = 10^{-3}$, $\tilde{k}_q = 1$, $\bar{k}_q = \text{Eq. (31)}$, $k_\delta = 10^{-3}$, $\tilde{k}_\omega = 20$, $\eta = 0.5$, $\gamma_i \forall i = 0.025$, $\mu = 0.1$, $\sigma = 10^{-3}$, $\hat{\mathbf{b}}(t_0) = \mathbf{0}_{3 \times 1}$, $\chi_i(t_0) \forall i = 0$. A time step of 0.025 sec was chosen with a total simulation time of 60 sec. An illustration of the quaternion, \mathbf{q} , and angular velocity, $\boldsymbol{\omega}$, is depicted in Fig (2). Notice that the states are driven to their desired values, \mathbf{q}_r and $\boldsymbol{\omega}_r$, respectively. Figure (3) shows the evolution of the cone angles, $\delta_i, \forall i = 1, 2, 3$. Despite actuator faults and a complete failure, the control and adaptive laws ensure constraint satisfaction for the entire duration. The designed control torque, $\boldsymbol{\tau}$, and the supplied torque, $\text{Tanh}(\boldsymbol{\tau})$, by the healthy actuators are indicated in Fig. (4). Notice that while $\boldsymbol{\tau}$ may violate the saturation constraints, the torque supplied to the actuators, $\text{Tanh}(\boldsymbol{\tau})$, remains within the constraint limit of 10 N-m. Moreover, after $t > 40$ sec, the control automatically compensates for the failed actuator.

REFERENCES

- Gao, S., Liu, X., Jing, Y., and Dimirovski, G.M. (2021a). Finite-time prescribed performance control for spacecraft attitude tracking. *IEEE/ASME Transactions on Mechatronics*.
- Gao, S., Liu, X., Jing, Y., and Dimirovski, G.M. (2021b). A novel finite-time prescribed performance control scheme

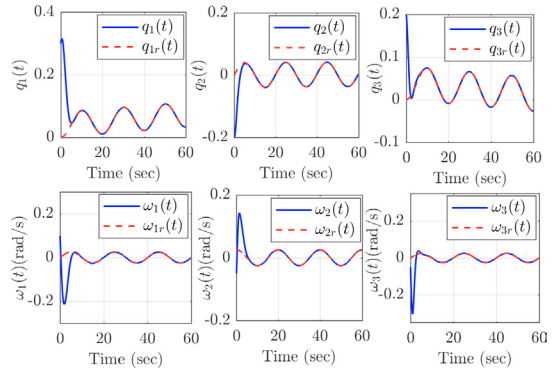


Figure 2. Evolution of \mathbf{q} and $\boldsymbol{\omega}$

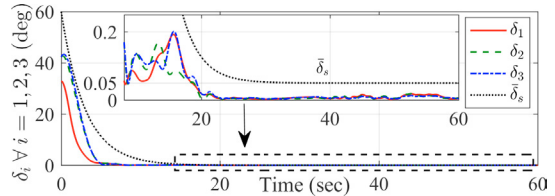


Figure 3. Evolution of $\delta_i \forall i = 1, 2, 3$ using BLF-based FTC.

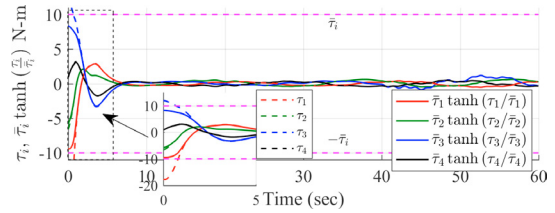


Figure 4. Evolution of $\boldsymbol{\tau}$ and $\text{Tanh}(\boldsymbol{\tau})$ - BLF-based FTC.

- for spacecraft attitude tracking. *Aerospace Science and Technology*, 118, 107044.
- Hou, L. and Sun, H. (2020). Anti-disturbance attitude control of flexible spacecraft with quantized states. *Aerospace Science and Technology*, 99, 105760.
- Hu, Q., Shao, X., Zhang, Y., and Guo, L. (2018). Nussbaum-type function-based attitude control of spacecraft with actuator saturation. *International Journal of Robust and Nonlinear Control*, 28(8), 2927–2949.
- Shao, X., Hu, Q., Shi, Y., and Jiang, B. (2018). Fault-tolerant prescribed performance attitude tracking control for spacecraft under input saturation. *IEEE Transactions on Control Systems Technology*, 28(2), 574–582.
- Tee, K.P., Ren, B., and Ge, S.S. (2011). Control of nonlinear systems with time-varying output constraints. *Automatica*, 47(11), 2511–2516.
- Thakur, D., Srikant, S., and Akella, M.R. (2015). Adaptive attitude-tracking control of spacecraft with uncertain time-varying inertia parameters. *Journal of guidance, control, and dynamics*, 38(1), 41–52.
- Vutukuri, S., Chakravarty, A., and Padhi, R. (2022). Time-varying quaternion constrained attitude control using barrier lyapunov function. In *2022 17th International Conference on Control, Automation, Robotics and Vision (ICARCV)*, 367–372. IEEE.
- Zhang, C., Xiao, B., Wu, J., and Li, B. (2021). On low-complexity control design to spacecraft attitude stabilization: An online-learning approach. *Aerospace Science and Technology*, 110, 106441.